Journal of the Korean Physical Society, Vol. 62, No. 1, January 2013, pp. 53∼58

Analysis and Modeling of the Optical Endpoint Signal for Precision Etching

Yong Jin Kim, Kyong Nam Kim and Geun Young Yeom*

Department of Advanced Materials Engineering, Sungkyunkwan University, Suwon 440-746, Korea

(Received 1 August 2012, in fianl form 26 November 2012)

Endpoint detection is an essential methodology for process control in dry etching for modern semiconductor manufacturing technology. In this paper, an analysis has been performed on the factors, such as the local etch rate, the local film thickness differences, and the open area and the global uniformities of the etch rate and film thickness, affecting the change in the optical emission endpoint signals on a patterned device wafer. Also, a model of the endpoint signal evolution, which includes an effective open ratio, the ratio of the relative open area after considering the local difference in the etch rate and the film thickness to the total open area at the very beginning of the etch process, has been established. Compared to the conventional open ratio, which is the ratio derived from the reticle used for lithography, the effective open ratio is better in explaining and predicting the endpoint signal change. The effective open ratio can be used to design dummy patterns that are used to improve endpoint detection in critical dry etch processes such as gate cuts in logic gate formation, *etc.*

PACS numbers: 52.77.Bn
Keywords: Endpoint detection, EPD, Patterned wafer etching, Modeling
DOI: 10.3938/jkps.62.53

I. INTRODUCTION

As the design rule for semiconductor devices shrinks to nanometer scale, complicated schematics for device fabrication, which require not only the development of high-performance process and equipment but the precise process control, have been introduced. The 'cut process' is one of example of a scheme requiring precise process control [1]. To fabricate smaller-area static, random access memory (SRAMs), narrow short-length gate lines are formed by cutting the narrow, long lines with small, open-area, bar-contact-type patterns. If precise control of the recess amount of conducting material beneath the mask dielectric is not possible in the cut etching of the mask dielectric, process excursions such as gate-oxide (GOX) pits occur gate conducting material is etched. In this respect, endpoint detection (EPD) for precise process control becomes more critical in modern semiconductor device fabrication.

Many research efforts were performed using various kinds of methodology such as electric signal monitoring, mass spectroscopy, optical interferometry, optical emission spectroscopy (OES) *etc.* [7-27]. The endpoint detection concept has also been utilized in the microelectronic fabrication other than dry etching, such as in-situ chamber cleaning of plasma-enhanced chemical vapor deposition (PECVD) equipment [2], a-Si:H removal by using H_2 plasma [3] *etc.* Interference signals obtained without an external light source were reported to be useful for endpoint detection for ion-beam etching [4]. Also, research using mass spectrometry was performed for the endpoint uniformity sensing and analysis [5].

In the case of conventional endpoint detection on a patterned wafer by using optical emission during the plasma etching, from the early stage of dry etch utilization in the semiconductor fabrication, endpoint detection for a small, open-area pattern has been studied [6] even though various factors affecting the endpoint signal were not examined thoroughly. In addition, many studies have been conducted to obtain endpoint signals with a high signal-to-noise ratio or to establish new techniques, resulting in endpoint signals different from traditional optical emission signals, especially for the small, open-area pattern. However, there are very few papers in which the factors determining the signal change, hence the possibility of the process endpoint detection itself, are investigated in detail for various processing situations. In this paper, analysis and modeling are suggested for the factors that determine the endpoint signal intensity change in optical emission spectroscopy, especially during the etching of patterned wafers.

*E-mail: gyyeom@skku.edu; Fax: +82-31-299-6565

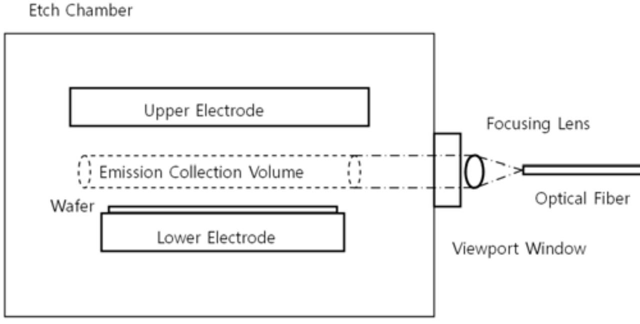

Fig. 1. Emissions from by-products molecules are collected by the focusing lens and enter an optical fiber through which they are delivered to the endpoint detection system.

II. MODELING AND ANALYSIS OF ENDPOINT SIGNAL

An endpoint signal is obtained by monitoring the emission intensity of by-products or etchant species. In every case, the emission intensity is proportional to the concentration of the corresponding species.

1. Model for the Number of By-product Molecules

Figure 1 shows the volume from which the emissions of by-products molecules are collected into the endpoint detection system via a lens and an optical fiber. The number of by-products molecules in the signal collection volume is determined by the balance between the generation on the wafer surface via etch reactions of the etchant and the material to be removed, and the loss by pumping out. The change in the number of by-products molecule number can be described as follows:

$$\frac{dN}{dt} = RAn\delta - \frac{N}{\tau}, \tag{1}$$

where N is the total number of by-products molecules, R is the etch rate, A is the total open area on the wafer surface where the material is being etched out, n is the number density of the material being etched, δ is the yield of by-products molecules per single etched material atom removal, and τ is the characteristic pumping time or residence time of the by-product molecules. Recent etch processes require highly anisotropic profiles, which implies no significant enlargement of the total open area and thus no significant contribution due to the generation of by-products from the surfaces of the sidewalls.

At steady state, *i.e.*, when the material being etched is exposed everywhere on the open area, $\frac{dN}{dt} = 0$ can be assumed. Figure 2 presents the etching amount at various etch times. The assumption of $\frac{dN}{dt} = 0$ can be used for the etch time when the etching layer is exposed everywhere such as in Fig. 2(a). In Fig. 2(b), at the etch time when the under-layer is exposed for fast-etch-rate patterns or for fast-etch-rate area, the number of by-products molecules will be different from that in Fig. 2(a), but the assumption of $\frac{dN}{dt} = 0$ still can be used with a decreased open area A. In Fig. 2(c), at the time when the under-layer is exposed everywhere, there will be no generation of by-products molecules, so the number of by-products molecules will decrease monotonically. Thus, for the etch times of Fig. 2(a) and 2(b), the total number of by-products molecules can be given as follows from the assumption of $\frac{dN}{dt} = 0$:

$$N = RAn\delta\tau, \tag{2}$$

Thus, the number of by-products molecules at steady state increases with increasing rate and open area, and the emission intensity, which has a linear dependency on the number of molecules increases with increasing etch rate and open area. This is a well-known characteristic of the optical endpoint signal.

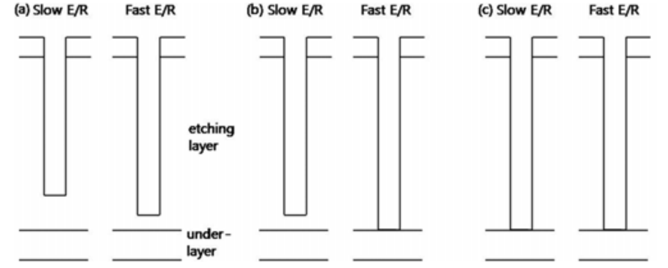

Fig. 2. Etch amount according to etch time: (a) before exposure of under-layer, (b) beginning of exposure of under-layer and (c) full exposure of under-layer.

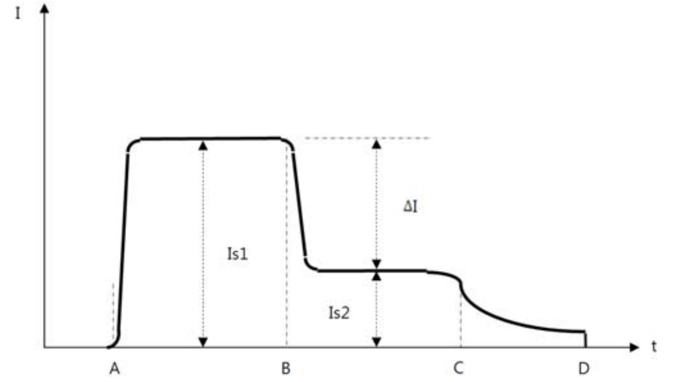

Fig. 3. Typical endpoint signal for Gate mask etching: A is RF power turn on, B and C and the 1st and the 2nd intensity decreases, respectively, and D is the RF power turn off.

2. Basic Analysis of Endpoint Signal

In Fig. 3, a typical endpoint signal obtained during the etching of a gate mask pattern wafer is shown. The

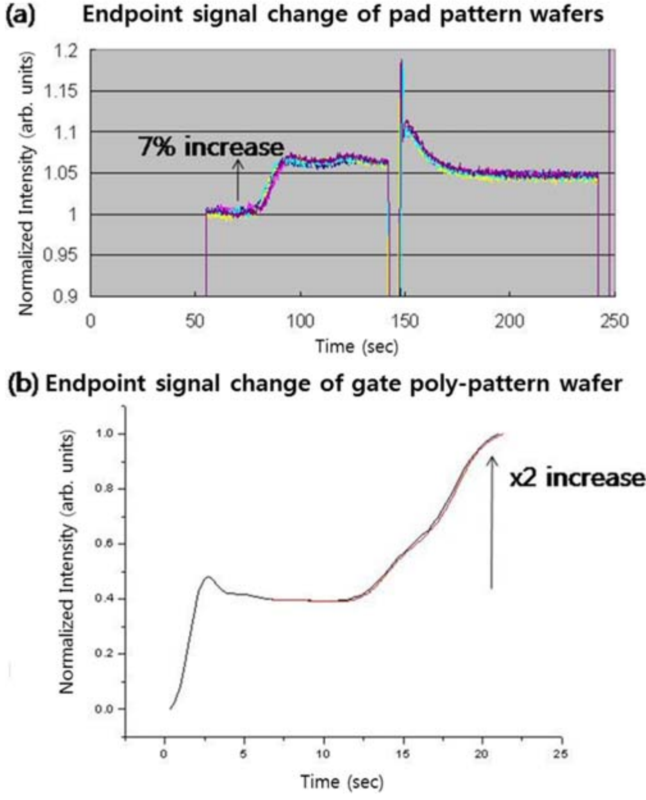

Fig. 4. (Color online) Endpoint signal changes at (a) pad pattern wafers and (b) gate poly-pattern wafers.

overall change in the endpoint signal intensity strongly depends on the pattern formed on the wafer. In the case of a gate pattern that has a large open area, the difference in the signal intensities before and after the endpoint becomes as high as several tens of percent. Conversely, in the case of a pad pattern that has a small open area, the difference in the signal intensities is as low as a few percent. These are displayed in Fig. 4.

At time A, the radio-frequency (RF) power is turned on, and a plasma is generated. The instantaneous formation of by-product molecules over the entire open surface results in a rapid increase in the corresponding emission intensity. For the time region A-B, the etch reaction and thus by-product formation occurs over the entire open surface on the wafer being etched. This time region A-B is the steady state during which the open area and the etch rate do not change: therefore, the generation of by-products molecules does not change, and the emission intensity is also constant.

At time B, even though the process conditions such as the RF power, pressure, gas flow rates, *etc.* are not changed, the emission intensity of by-product molecules decreases. This decrease comes from the decrease in the total area for by-product molecule generation because, at a certain position on the wafer, the material being etched is removed and the underlying layer material starts to be exposed. As the open area where the underlying layer is

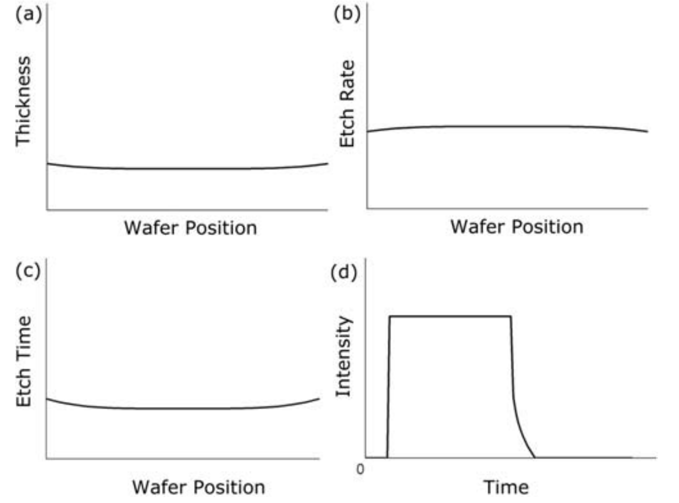

Fig. 5. EPD intensity signal according to global uniformity: (a) material thickness, (b) etch rate, and (c) etch time as functions of wafer position of the wafer being etched. (d) shows the temporal change of the optical emission intensity of the by-product molecule.

exposed becomes larger, the area of the material current by being etched gets smaller, which results in a gradual decrease in the emission intensity of the by-product molecules. This can be clearly seen in Fig. 5.

The global uniformity or the distribution of the film thickness and the etch rate can be given Figs. 5(a) and (b), respectively. The etch rate is well known to be linearly proportional to the product of the plasma density, the bias voltage and the etchant radical flux density. The plasma density has a uniform distribution on the wafer surface, but, the neutral etchant flux has a distribution where uniformity is worse than that of the plasma density, so a conventional dry etcher has an etch-rate uniformity of a few percent, which can be represented as the distribution shown at Fig. 5(b).

If the distribution functions of the thickness and the etch rate at wafer position r are denoted as $\Theta(r)$ and $R(r)$, respectively, the removal time of the material being etched at r, $T(r)$, can be calculated simply as $T(r) = \Theta(r)/R(r)$, which is displayed in Fig. 5(c). The by-product molecule generation at a wafer position r will continue as long as material to be etched exist, *i.e.*, as long as the process time does not exceed the removal time of the material, that is, for $t < T(r)$. A step-function-like contribution function can be introduced as $S(r,t)$ to account for the emission intensity at a wafer position:

$$S(r,t) = \left\{ \begin{array}{l} 1, t < T(r) \\ 0, t \geq T(r). \end{array} \right\} \tag{3}$$

The temporal change in the emission intensity of the by-product molecules can be derived from the accumulation of the contribution from the entire wafer as follows:

$$I(t) = \int_{\Omega} i(r) S(r,t) dr, \tag{4}$$

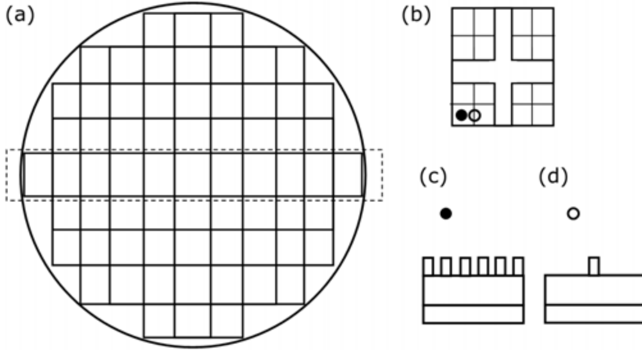

Fig. 6. Open size difference at different positions on a chip: (a) patterned wafer and the collection volume of the emission for the EPD system (dotted box), and (b) a simplified structure of the pattern in a photo shot composed of dense pattern blocks (c) and (d) a sparse pattern.

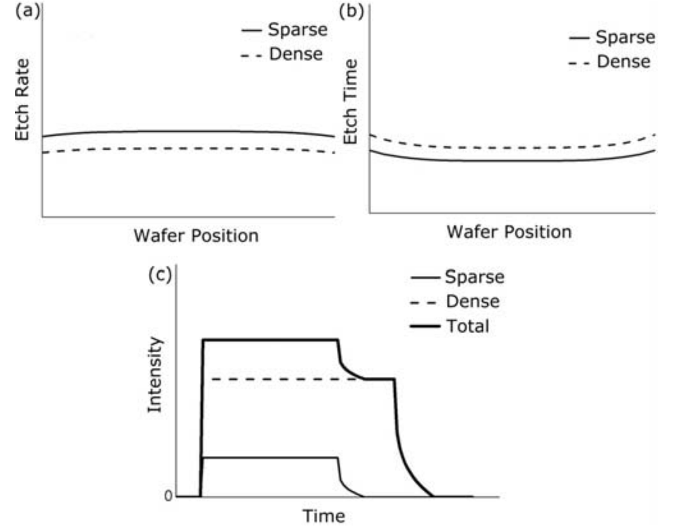

Fig. 7. For sparse and dense patterns, (a) etch rates, (b) etch or removal time, and (c) respective emission intensity changes.

where Ω is the volume for the intensity accumulation and $i(r)$ is the emission at the wafer position r, where $i(r) = kn_e(r)N(r)$ is determined from the electron density $n_e(r)$ and the by-product molecule density $N(r)$. With the given profiles of the film thickness and the etch rate, $\Theta(r)$ and $R(r)$, and thus the removal time, $T(r)$, the temporal change in the emission intensity of the by-product molecules is shown in Fig. 5(d).

In the usual case of commercially-acceptable uniformity of the film thickness and the etch rate, the emission intensity change shows a rapid decrease at the process time when almost all the material to be etched has been removed. After all the material to be etched has been removed, the emission intensity of the by-product molecules goes to zero after the characteristic residence time. However, as can be seen in Fig. 4, the 2nd flat intensity region exists after the intensity decrease following the 1st steady-state intensity. This 2nd flat intensity region is caused by local differences in the etch rate and the film thickness.

3. Analysis of Endpoint Signal by Using the Differences in Local etch rates and Film Thicknesses

In Fig. 6(a), a patterned wafer is drawn schematically. Exactly the same pattern from the reticle is repeated over the entire wafer by using photo-lithography. The collection volume of the emission for the EPD system is drawn as a dashed box. In Fig. 6(b), a simplified structure of the pattern in a shot is displayed. It is composed of dense-pattern blocks and separating regions where sparse patterns exist, as shown in Figs. 6(c) and (d), respectively.

The etch rate in a sparse pattern is well known to be higher than that in a dense pattern in the gate etch process. Thus, the endpoint signal emitted from the by-product molecules is affected not only by the global uniformity but also by this local etch rate difference. From the local differences in the etch rates caused by the pattern density, the open area in the wafer can be considered to be shrunk. That is, even at the time when the material being etched is entirely removed at the sparse patterns, some of the material being etched still remains at the dense patterns, so the change in the endpoint signal comes only from the removal of the material being etched at the sparse patterns. In Fig. 4, the intensity of the optical emission coming from the dense pattern with the lower etch rate corresponds to the 2nd flat value in the region B-C. The endpoint signal intensity, I_{s2}, is determined by using the open area of the dense patterns while the 2nd flat signal time, t_{BC}, is related to the etch time of the material remaining at the dense patterns. Thus, if the ratio of the sparse patterns to the whole open area is known, the intensity change, ΔI, can be estimated.

The profiles of etch rates across the wafer can be assumed to be those in Fig. 7(a), where a higher etch rate at each position corresponds to a sparse pattern and a lower etch rate to a dense one. By assuming that the film thickness is uniform globally, the etch-time profiles for the respective patterns show an offset in Fig. 7(b). In the case of two different pattern densities and thus etch rates, the overall emission intensity accumulated in the endpoint system can be derived as the sum of the contributions from the two patterns:

$$I(t) = \int_{\Omega} [i_S(r)S_S(r,t) + i_D(r)S_D(r,t)]\, dr. \tag{5}$$

In the endpoint signal simulated for the case of local etch-rate difference, two flat regions are observed as shown in Fig. 7(c). The 1st flat intensity value corresponds to the entire open area while the 2nd flat intensity comes from the low-etch-rate pattern. Thus, if the area ratios for the different etch rate patterns are known, estimat-

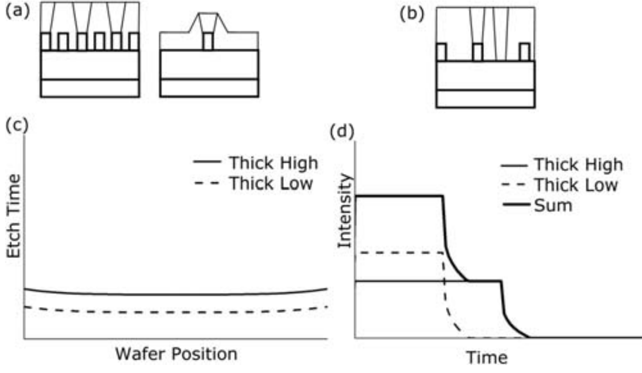

Fig. 8. Various cases of local thickness or depth differences of the material to be etched: (a) as-deposited thickness difference due to the underlying pattern density, (b) film deposition followed by chemical mechanical polishing (CMP) process and simultaneous contact formation on gate and active regions, which results in an etch depth difference among the contact holes, (c) etch time differences to the endpoint due to the differences in the local thicknesses or depths, and (d) resultant endpoint signal.

ing the endpoint signal intensity change at the moment when the material at high-etch-rate pattern is entirely removed all while the etch reaction and by-product generation continues at the low-etch-rate pattern is possible. Conversely, the area ratio of the low-etch-rate pattern to the entire open area can be estimated from the endpoint signal change. The etch time for the first drop of the endpoint signal is determined by the etch rate of the sparse pattern while the etch time for the second drop is determined by the low dense pattern etch rate. Hence, from the two respective etch times, the ratio of the etch rates at two different density patterns can be estimated. For example, if the etch rate at the dense pattern is 70% that at the sparse pattern and the ratio of the dense pattern to the whole open area is 75%, then the resulting endpoint signal intensity decreases about 25%, and the time of 2nd intensity region is about 43% of the time of the 1st intensity region.

The analysis of the endpoint signal in the case of local thickness differences can be performed in a similar way. Local thickness differences occur during dielectric film deposition with a varying underlying pattern density. Also, there is a contact-etching process in which the contact depth varies with the location where the contact hole is formed. These cases are shown in Figs. 8(a) and (b), respectively. The etch time to the endpoint will be higher for a thicker local thickness as shown in Fig. 8(c): therefore, the resulting endpoint signal resembles that of the local etch-rate-difference case, as shown in Fig. 8(d).

From analyses of the optical emission endpoint signals in the cases of local-etch-rate and thickness differences, as well as global uniformity considerations, we can suggest that the literal open area is not enough to explain or predict a realistic endpoint signal. Hence, an effective open ratio, which can be defined as the ratio of the area with a different etch rate or thickness to the entire open area at the very beginning of the etch process, is suggested.

4. Effective Open Ratio

The possibility of endpoint detection at the interface of two layers is mainly determined by the amount of signal change at that point. Although the signal intensity itself is a function of the total open area during the etching of the first layer, the change in the signal intensity strongly depends on the change in the area where the material being etched remains. If various types of patterns with different etch rates are considered, the continuity equation of the by-product molecules would be modified as follows:

$$\frac{dN}{dt} = n\delta \sum_i R_i A_i - \frac{N}{\tau}, \tag{6}$$

where R_i is the etch rate at the pattern with open area A_i. If we introduce the open ratio $\gamma_i \equiv A_i/A$, the equation can be rewritten as follows:

$$\frac{dN}{dt} = An\delta \sum_i R_i \gamma_i - \frac{N}{\tau}. \tag{7}$$

For a two-pattern case composed of a sparse pattern and a dense pattern, therefore, in the gate-pattern etching composed of fast and slow etch rates, the effective open ratio, which is the open ratio of the fast etch rate, *i.e.*, the sparse pattern density, to the whole open area, will be a good index for the change in the number of molecules or the endpoint signal intensity:

$$\frac{dN}{dt} = An\delta\left[R_S\gamma + R_D(1-\gamma)\right] - \frac{N}{\tau}, \tag{8}$$

$$N = \begin{cases} An\delta\left[R_s\gamma + R_D(1-\gamma)\right], & t < T \\ An\delta R_D(1-\gamma), & t \geq T \end{cases}, \tag{9}$$

where T denotes the time when all the sparse pattern or the high-etch-rate pattern is etched out. From this, the endpoint signal change, which is proportional to the change in the number of by-products molecule, shows a linear dependence on the effective open ratio:

$$\Delta I \propto \Delta N = N(t < T) - N(t \geq T) = An\delta\gamma R_S. \tag{10}$$

III. CONCLUSION

In nanometer-scale semiconductor device fabrication, endpoint detection in the dry etching process is very critical. Thus, dummy patterns to enlarge the endpoint signal change are often inserted in the layout drawing. However, without careful considerations of the local etch rates or depth differences, it may not result in the wanted

endpoint signal improvement. In this paper, a modeling and analysis for the optical endpoint signal are suggested, and the effective open ratio, the area ratio of the short-removal-time pattern to the whole pattern, is proposed as a promising index for the endpoint signal change.

ACKNOWLEDGMENTS

This work was supported by the Industrial Strategic Technology Development Program (10041681, Development of fundamental technology for 10 nm process semiconductor and 10 G size large area process with high plasma density and VHF condition and KI002182, TFT backplane technology for next generation display) funded by the Ministry of Knowledge Economy (MKE, Korea). This work was also supported in part by the World Class University program of the National Research Foundation of Korea (Grant No. R32-2008-000-10124-0).

REFERENCES

[1] V. S. Basker *et al.*, in *Symposium on VLSI Technology* (Hsinchu, Taiwan, April 26-28, 2010), p. 19.

[2] M. Gallagher, C. Ebel, J. Fournier, T. Weeks, G. MacDougall, T. Knotts, C. Lam and K. Peterson, in *Advanced Semiconductor Manufacturing Conference and Workshop* (Cambridge, Massachusetts, November 12-14, 1996), p. 333.

[3] H. H. Yue, S. J. Qin, J. Wiseman and A. Toprac, J. Vac. Sci. Technol., A **19**, 66 (2001).

[4] F. Heinrich, H-P. Stoll and H-C. Scheer, Appl. Phys. Lett. **55**, 1474 (1989).

[5] H. Ren, J. Wu, J. Yan, J. Zhang and W. Wang, in *Intelligent Information Technology Application* (Nanchang, China, November 21-22 2009), p. 377.

[6] L. Hsu, in *International Symposium for Semiconductor Manufacturing* (Tokyo, Japan, September 27-29, 2004), p. 111.

[7] R. Jaiswal, I. Sim, A. Jain, T. Q. Chen, L. Meng and Y. Pradeep, in *International Symposium for Semiconductor Manufacturing* (San Jose, California, September 30-October 2, 2003), p. 370.

[8] N. Layadi, T. Lill, J. Trevor, S. J. Molloy, F. Baumann, M. N. Grimbergen, T. C. Esry and J. Chinn, in *Advanced semiconductor Manufacturing Conference and Workshop* (Boston, Massachusetts, September 8-10, 1999), p. 227.

[9] C. H. Low, W. S. Chin, M. S. Zhou, S. T. Loong and L. Chan, in *IEEE Interconnect Technology Conference* (Irvine, California, June 1-3, 1998), p. 265.

[10] M. D. Baker, C. D. Himmel and G. S. May, IEEE Trans. Compon. Packag. Manuf. Technol. Part A **18**, 478 (1995).

[11] M. W. Kim, S. G. Kim, S. Zhao, S. J. Hong and S. S. Han, ECS Trans. **34**, 943 (2011).

[12] E. Ragnoli, S. McLoone, J. Ringwood and N. Macgerailt, in *Advanced Semiconductor Manufacturing Conference* (Boston, Massachusetts, 5-7 May 2008), p. 156.

[13] T. Reis, in *IEEE Advanced Semiconductor Manufacturing Conference* (Santa Carla, California, April 23-24, 2001), p. 55.

[14] E. A. Rietman and N. Layadi, IEEE Trans. Semicond. Manuf. **13**, 457 (2000).

[15] E. A. Rietman, J. T.-C. Lee and N. Layadi, J. Vac. Sci. Technol., A **16**, 1449 (1998).

[16] E. A. Rietman, N. Layadi and S. W. Downey, J. Vac. Sci. Technol., B **18**, 2500 (2000).

[17] J. P. Roland, J. Vac. Sci. Technol., A **3**, 631 (1985).

[18] H. C. Sun, V. Patel, B. Singh, C. K. Ng and E. A. Whittaker, Appl. Phys. Lett. **64**, 2779 (1994).

[19] L. Tao, A. P. Yalin and N. Yamamoto, Rev. Sci. Instrum. **79**, 115107 (2008).

[20] S. Thomas III, H. H. Chen and S. W. Pang, J. Vac. Sci. Technol., B **15**, 681 (1997).

[21] B. H. Boo, J. Korean Phys. Soc. **59**, 3205 (2011).

[22] J. R. Ahn, S. G. Lee and C. J. Park, J. Korean Phys. Soc. **59**, 2670 (2011).

[23] B. Ji, J. H. Yang, P. R. Badowski and E. J. Karwacki, J. Appl. Phys. **95**, 4452 (2004).

[24] H. C. Neitzert, W. Hirsch and M. Kunst, J. Appl. Phys. **73**, 7446 (1993).

[25] F. Heinrich, H-P. Stoll and H-C. Scheer, Appl. Phys. Lett. **55**, 1474 (1989).

[26] J. J. Chambers, K. Min and G. N. Parsons, J. Vac. Sci. Technol., B **16**, 2996 (1998).

[27] G. Chang, J. P. McVittie, J. T. Walker and R. W. Dutton, IEEE Electron Device Lett. **5**, 514 (1984).